Ultra-broadband THz field detection by ion-implanted III-V PC Antenna

Ci-Ling Pan

Department of Photonics and Institute of Electro-Optic Engineering
National Chiao Tung University 1001 Ta-Hsueh Rd., Hsinchu, Taiwan 30010, R.O.C.
contact: clpan@faculty.nctu.edu.tw

ABSTRACT

The photoconductive (PC) antenna fabricated on arsenic-ion-implanted GaAs (GaAs:As^+) and proton-bombarded InP (InP:H^+) substrates are shown to have a useful detection bandwidths beyond 30 THz. This is comparable to that of the reference LT-GaAs PC antenna. The signal-to-noise ratio of these ion-implanted III-V PC antennas are, however, worse than that of the LT-GaAs devices because of the higher stray currents of the former under illumination. Ion-implanted III-V PC antennas are nevertheless attractive because the implanters are widely available, process parameters well-established and compatible with the IC industry. Implantations in selective areas are also straight forward. Our results suggest that ion-implanted III-V material can be a good choice as substrate or THz PC antennas, if the resistivity is increased by a proper annealing process and/or optimizing the implantation recipe.

Keywords: THz radiation, detection, Arsenic-ion-implanted GaAs, proton-bombarded InP, III-V, photoconductive antenna

INTRODUCTION

Photoconductive (PC) antennas gated with ultrashort optical pulses have been widely used as highly efficient emitters and detectors for terahertz (THz) pulsed radiation. The useful bandwidths of typical PC antennas were several THz.[1,2] The limited bandwidth of PC antennas was explained by the finite carrier lifetime or the momentum relaxation time of the carriers in the PC substrates. This was extended up to 60 THz by Kono *et al.*[3-5] using sub-20 fs laser pulses, low-temperature-grown GaAs (LT-GaAs) PC antennas and a collinear geometry for THz and gating beams for excitation. Device-quality LT-GaAs, however, are still hard to come by. Alternatively, one can prepare photoconductive substrates by ion-implantation. Implanters are widely available and the process reasonably reproducible. Arsenic-ion-implanted GaAs (GaAs: As^+)[6] exhibits structural, electrical, and ultrafast optoelectronic characteristics strikingly similar to those of LT-GaAs,[7] and is expected to work as an efficient PC substrate as LT-GaAs. On the other hand, InP potentially can be an alternative to GaAs as the PC substrate material. Indeed, a PC antenna fabricated on semi-insulating InP (SI-InP) showed a higher responsivity and a SNR larger 2 times larger than those of a LT-GaAs device in a regime of very weak probe laser power (~ 1 μW), although at higher probe power the LT-GaAs PC antenna out-performed the SI-InP one.[8] The degradation of SNR of SI-InP PC antenna at high probe laser power was attributed to PC saturation associated with the long carrier lifetime of InP (τ_{eff} ~70 ps). Low-temperature grown InP (LT-InP) was reported by Liang et al.[9] However, LT-InP was highly conductive, because of the n-type conductivity originating from the abundant presence of P_{In} antisites. Therefore, InP can be a good candidate as the PC substrate if it is sufficiently resistive and the carrier lifetime was shortened to that of LT-GaAs (~ 1 ps). This can accomplished through ion-implantation. Lamprecht *et al.*[10] observed ultrashort carrier lifetimes in proton-bombarded InP (InP: H^+), which decreased monotonically with the dosage and was as short as 95 fs at the highest dosage (1×10^{16} cm^{-2}). Messner *et al.*[11] also showed that the photo-excited electron lifetime in InP: H^+ became less than a picosecond for proton dosages around $5x10^{15}$ cm^{-2}. The implantation depth of the protons in InP was estimated to be about 1.5 μm from the surface.[8]

Recently, we have shown that photoconductive (PC) antenna fabricated on arsenic-ion-implanted GaAs (GaAs:As^+) and proton-bombarded InP (InP:H^+) substrates have a useful detection bandwidths beyond 30 THz[12,13]. In this paper, the key performance of these ion-implanted III-V THz antennas, e.g., the bandwidth and SNR, as compared to those of an LT-GaAs one and discussed in relation to the photoconductive gain and resistivity.

Ultrafast Phenomena in Semiconductors and Nanostructure Materials IX,
edited by Kong-Thon Tsen, Jin-Joo Song, Hongxing Jiang, Proc. of SPIE Vol. 5725
(SPIE, Bellingham, WA, 2005) · 0277-786X/05/$15 · doi: 10.1117/12.596668

Downloaded From: http://proceedings.spiedigitallibrary.org/ on 04/26/2014 Terms of Use: http://spiedl.org/terms

EXPERIMENTAL METHODS

We employ a mode-locked Ti: sapphire laser ($\lambda \approx 800$nm), generating a 15-fs (the spectral width was 95 nm or ~ 47 THz) pulse train at 75 MHz and an average output power of 400 mW. Pump beam was focused onto a 10-μm-thick (110) ZnTe crystal bonded on a 1-mm-thick fused silica plate by a gold-coated off-axis parabolic mirror with a focal length (f) of 50 mm to generate broadband THz radiation by the optical rectification effect. THz beam emitted from the ZnTe emitter was then collimated and focused onto the PC antenna by a pair of off-axis parabolic mirrors (f=50 mm). The average pump power on the ZnTe emitter was 150 mW after mechanical chopping at 2 kHz. The gating laser power was 23 mW. The GaAs:As^+ substrate was prepared by implanting the semi-insulating (SI) GaAs substrate with arsenic ions at a total doses of 10^{16} ions/cm^2 with multiple energies of 50keV, 100keV and 200keV. This was followed by furnace annealing at 600 °C for 30 minutes. The ion implantation depth was estimated to be about 100 nm by SIMS (Secondary Ion Mass Spectroscopy) measurement. Four InP: H^+ PC antennas were prepared by bombarding (100)-oriented SI-InP substrates with 180 keV proton with dosages of 1×10^{15}, 3×10^{15}, 1×10^{16} and 3×10^{16} ions/cm^2, respectively. The LT-GaAs sample used as the reference was grown at a substrate temperature of 250 °C by molecular beam epitaxy and annealed at 600 °C for 5 min after growth. The carrier lifetime of GaAs:As^+ samples were estimated to be around 1~2 ps by a transient photo-reflectance measurement (see Fig. 2). The carrier lifetimes of all InP: H^+ and LT-GaAs samples used in this experiment were also found to be shorter than 2 ps. A micro-stripline dipole antenna was fabricated on each InP:H^+ wafer by standard cleaning, metallization and lift-off procedures for InP. During the metallization processes, Ni-Ge-Au-Ge-Ni-Au metal layers were evaporated and annealed at around 400°C. The antenna consisted of 5-μm-wide coplanar striplines (6-mm long) separated by 20-μm and contacts, rectangular in shape, at the center of the coplanar striplines. The contact width and length (in vertical direction to the striplines) were 10 μm and 7.5 μm, respectively. The PC gap between the contacts was 5 μm.

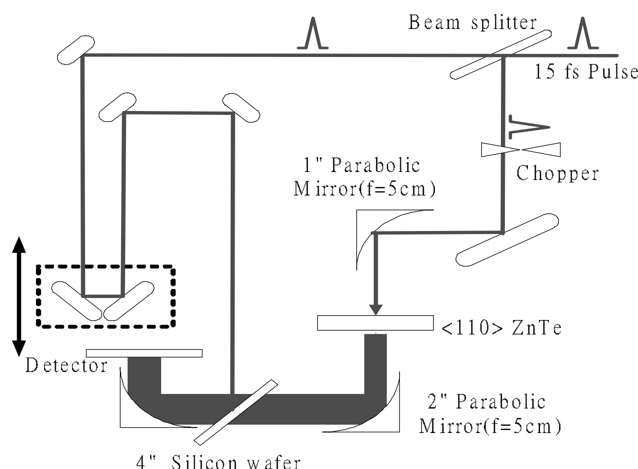

Fig.1 A schematic of the Experimental set-up for broadband THz detection.

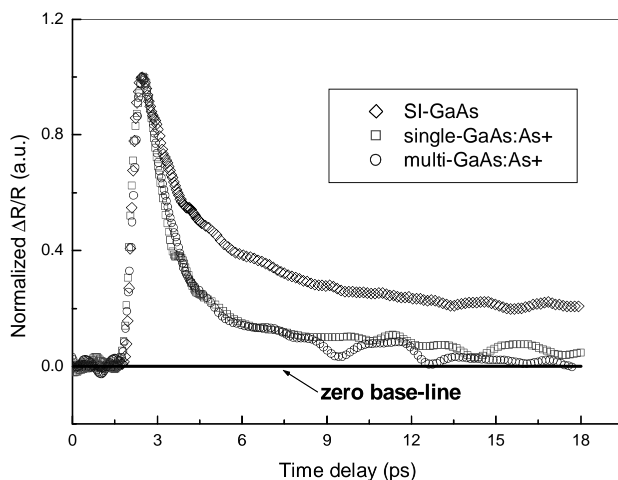

Fig.2 Normalized transient photoreflectance of single- and multiple-arsenic-ion-implanted GaAs with that of semi-insulating (SI) GaAs.

RESULTS AND DISCUSSIONS

Downloaded From: http://proceedings.spiedigitallibrary.org/ on 04/26/2014 Terms of Use: http://spiedl.org/terms

Figure 3 shows the current-voltage (I-V) measurement (a) without and (b) with the laser excitation (23 mW) for the GaAs:As^+, LT-GaAs and SI-GaAs PC gap (5 µm) in a weak bias region. SI-GaAs and LT-GaAs PC gaps show

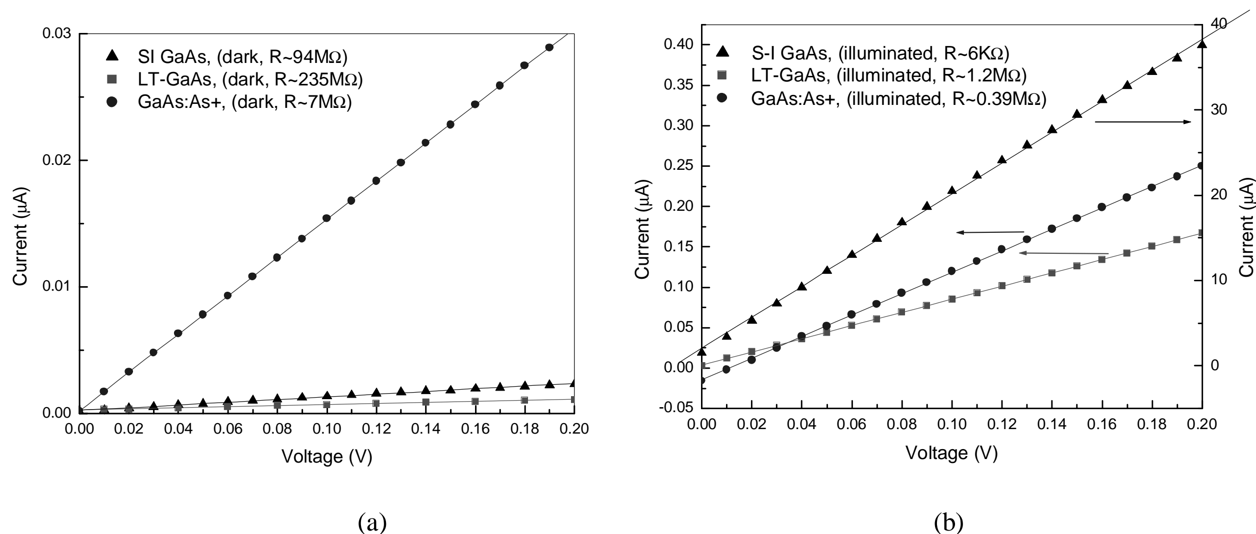

(a) (b)

Fig.3 Current-voltage (I-V) measurements (a) without and (b) with laser irradiation for GaAs: As^+ (circle dot), SI-GaAs (triangular dot) and LT-GaAs (square dot) PC gap (5µm) antennas near zero bias region. The resistance (R) estimated from the slope is indicated in each diagram.

lower dark current. The resistance of LT-GaAs, GaAs:As^+ and SI-GaAs PC gaps decreased to about 1.2MΩ, 0.4MΩ and 6KΩ, respectively, by the laser irradiation. The significant decrease from the high dark resistance (~100 MΩ) to the low photoconductive resistance (6 kΩ) in the SI-GaAs gap indicates a large PC gain, which is attributed to the long carrier lifetime. The LT-GaAs gap showed the highest dark resistance. However, its photoconductive resistance was also high (low PC gain), which is attributed to the short carrier lifetime (~ 1 ps). On the other hand, GaAs:As^+ showed the lowest dark resistance, while it showed slightly lower PC resistance (higher PC gain) than that of LT-GaAs (about one third of LT-GaAs). The lower PC resistance of GaAs:As^+ compared to that of LT-GaAs is attributed to the slightly longer carrier life time (~ 2 ps) and a contribution from the non-ion-implanted SI-GaAs substrate, which has a much lower photoconductive resistance than the As^+-ion implanted layer. We observed significant stray currents in all antennas at the zero bias condition, which may contribute to the noise in THz signal detection; The stray current from SI-GaAs, GaAs:As^+ and LT-GaAs were about 1.5 µA, 16 nA and 3 nA, respectively, at the gating power of 23 mW. The origin of the stray currents seems to be the asymmetric Schottky behavior at the metal-semiconductor contact. For dark I-V dependence, such Schottky characteristic is difficult to observe because of relatively high resistivity of the substrate. On the other hand, when we photo-excite the gap with the laser, increasing the conductivity, the Schottky characteristics of the contact become more clear, as observed in the I-V dependence with 23 mW excitation of the PC gap, which showed non-zero crossing at the V=0 axis (the vertical axis). Therefore, the high noise level observed in GaAs:As^+ antenna is attributed to the asymmetric Schottky characteristics of the metal-semiconductor contacts in the photo-excited condition.

Figure 4 shows the signal waveforms detected by the (a) GaAs: As^+, (b) SI- GaAs and (c) LT-GaAs PC antennas for THz radiation generated from the ZnTe emitter. THz waveform detected with the SI-GaAs antenna was averaged for three sequential scanning of the delay stage with a lock-in amplifier constant of 0.3 sec, while for the other PC antennas the scanning was only once. The detected peak signal current from GaAs:As^+, SI GaAs and LT-GaAs PC antennas was 0.02 nA,0.3 nA and 0.24 nA, respectively. The signal to noise ratio (SNR) was estimated to be about 20, <10 and 100, respectively. The signal current detected with the GaAs: As^+ PC antenna was lower than the other two types PC antennas by one order, while the noise level was comparable to that with the LT-GaAs PC antenna. The low signal in the GaAs: As^+ PC antenna is attributed to the insufficient thickness of the arsenic ion-implanted layer, which was only 10% of the absorption depth (~ 1µm) at the excitation laser wavelength; Most of the carriers excited in SI-

Downloaded From: http://proceedings.spiedigitallibrary.org/ on 04/26/2014 Terms of Use: http://spiedl.org/terms

GaAs substrate beneath the ion-implanted layer could not contribute to the signal since after the photoconductive decay in As^{+}-ion-implanted layer, the long-lived carriers in non-ion-implanted SI-GaAs are blocked to flow into the antenna contact by the insulating layer. The SNR of SI-GaAs PC antenna was lowest, although the signal current level was the highest. The low SNR of SI-GaAs PC antenna is attributed to the large current noise originating from the long-lived photo-exited carriers (lifetime > 100 ps), while the other two have carrier lifetimes of 1~2 ps.

Figure 5 shows Fourier transformed amplitude spectra of the THz waveforms shown in Fig. 4. The spectral profiles are almost the same for the three cases. The high frequency end of the spectral distribution is extending to about 30 THz. The end of the spectral distribution above the noise floor was estimated to be 32 THz and 24THz for GaAs:As^{+} and SI-GaAs PC antenna, respectively (40 THz for LT-GaAs PC antenna), which are the highest frequencies reported so far for the same kind of PC antennas. The spectral bandwidth was limited by the cut off frequency (~40 THz) due to the phase-mismatch between the THz radiation and pump laser pulse in the 10-um thick ZnTe emitter.[3] Characteristics of the three type of PC antennas are summarized in Table 1.

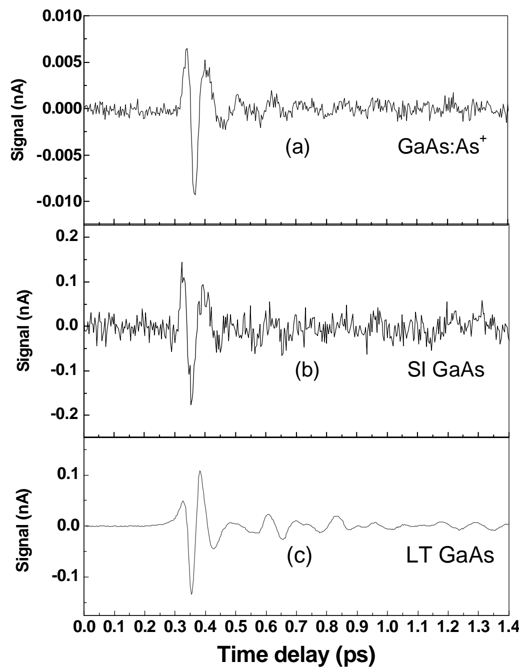

Fig.4 Time-resolved THz radiation waveforms detected by PC antenna based on (a) GaAs:As^{+} ,(b) SI-GaAs and (C) LT-GaAs. The emitter was a 10-μm thick (110) ZnTe crystal.

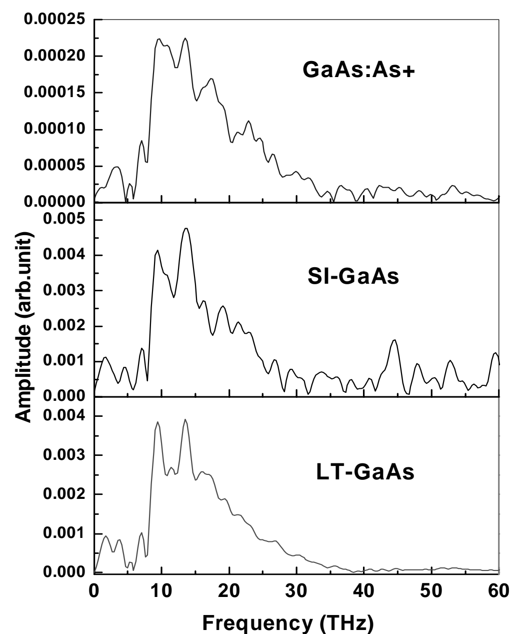

Fig.5 Fourier transformed amplitude spectra of the PC-detected THz waveforms shown in Fig. 4.

Table 1 Comparison of characteristics of GaAs: As^{+} with LT-GaAs and SI-GaAs PC antenna detectors.

	LT-GaAs	SI-GaAs	GaAs: As^{+}
Resistance (R) (Dark)	235MΩ	> 100 Ω	6 MΩ
Resistance (R)	1.2 MΩ	3 kΩ	0.33 MΩ

Downloaded From: http://proceedings.spiedigitallibrary.org/ on 04/26/2014 Terms of Use: http://spiedl.org/terms

(23mW illumination)			
Detected peak signal	0.24 nA	0.3 nA	0.02 nA
Detectable bandwidth	40THz	23THz	33THz
SNR	100	< 10	20
Noise level (arb. Unit)	1	~ 50	~ 1

Figure 6 shows the current-voltage (I-V) characteristics for InP: H^+ and LT-GaAs PC gaps at nearly zero bias (< 0.2 V) without and with laser excitation. The linear I-V characteristics observed in the measurements for the four samples near zero bias field suggests that there should be no significant Schottky barrier effect, which can reduce the signal current due to the THz field biasing the PC antenna.[8] The resistance of the InP: H^+ PC gaps, which decreased as the ion dosage increased except for the case of 3×10^{16} ions/cm^2, and the LT-GaAs one are summarized in Table 1. The decreasing trend for InP: H^+ can be explained by the presence of the shallow defects, as our InP: H^+ samples were not annealed after the proton bombardment.[14] The resistance of InP: H^+ with the highest dosage (3×10^{16} ions/cm^2) was 4 times larger than other InP: H^+ samples. It was reported that the resistance of InP: H^+ increased through annealing.[14] We thus tentatively attribute this increase in resistance to the self-annealing effect of implantation, by which the shallow defects were reduced at the highest dosage. It has also been demonstrated that annealing can reduce the defect density on arsenic-ion-implanted GaAs.[15] By the self-annealing mechanism, the shallow defect density might have also reduced in InP: H^+ prepared at the highest dosage. The stray current from InP: H^+ at dosages of 1×10^{15}, 3×10^{15}, 1×10^{16}, 3×10^{16} ions/cm^2 and LT-GaAs PC antennas were about 300 nA, 400 nA, 872 nA, 85 nA and 10 nA, respectively, at a gating power of 23 mW. The high conductance and the relatively low stray current of the InP: H^+ substrate with a dosage of 10^{15} ions/cm^2 implied a high responsivity and low noise.

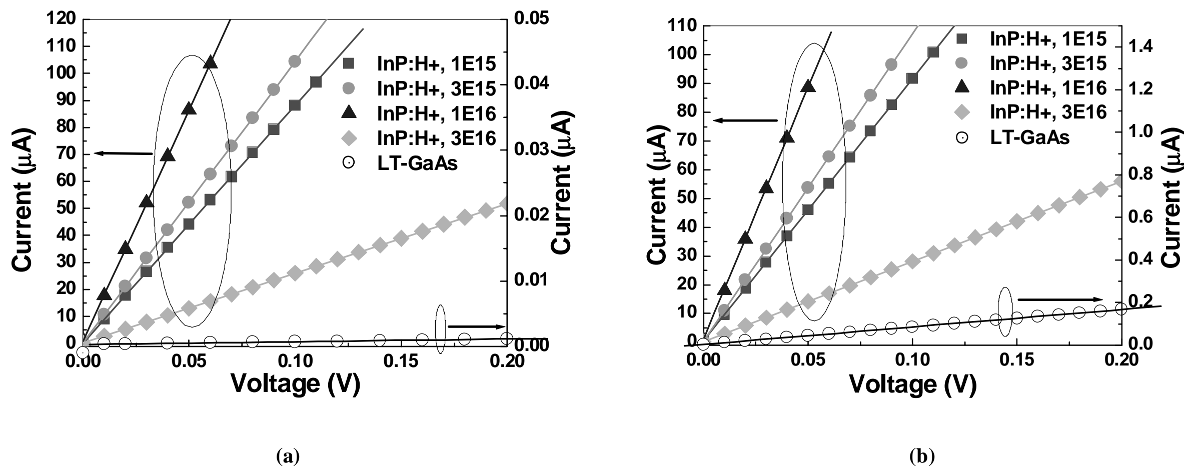

Fig. 6. Current-voltage (I-V) measurement (a) without and (b) with optical illumination for InP: H^+, doses of 10^{15} (square dot), 3×10^{15} (circle dot), 10^{16} (triangular dot), 3×10^{16} (diamond dot) ions/cm^2 and LT-GaAs (open circle) PC antennas with 5 μm gap in the weak bias case.

Table 2. Comparison of characteristics PC antenna detectors.

	LT-GaAs	**InP: H^+(1x10^{15})**	**InP: H^+(3x10^{15})**	**InP: H^+(1x10^{16})**	**InP: H^+(3x10^{16})**
Resistance (R) (Dark)	235MΩ	1.1 kΩ	0.97 kΩ	0.579 kΩ	3.8 kΩ
Resistance (R) (23mW illumination)	1.2 MΩ	1.07 kΩ	0.93 kΩ	0.568 kΩ	3.4 kΩ

Downloaded From: http://proceedings.spiedigitallibrary.org/ on 04/26/2014 Terms of Use: http://spiedl.org/terms

Detected peak signal	0.24 nA	0.27 nA	0.15 nA	0.079 nA	0.082 nA
Detectable bandwidth	40THz	33THz	33THz	24THz	33THz
SNR	100	50	26	<12	40
Noise level	1	6.19	6.36	7.62	2.25

The THz waveforms detected by each InP: H^+ and the LT-GaAs PC antenna are shown in Fig. 7(a). The detected THz peak signal currents are also listed in Table 2. The signal amplitudes in InP: H^+ PC antennas are all larger than the GaAs:As^+ device.[12] They are, however, in general lower than that of the LT-GaAs PC antenna except for the 1×10^{15} ions/cm^2 case. The decreasing trend and saturation in PC response with dosage has also been observed in PC switches fabricated on GaAs:As^+.[15] Figure 7(b) illustrates the Fourier transformed spectra of the PC-detected THz waveforms. The sharp spectral peaks around 9 THz and 10.4 THz observed for the LT-GaAs and InP: H^+ PC antenna, respectively, correspond to the LO-phonon frequencies of the substrates. The peaks are attributed to the optical phonon resonance effect: Near the LO-phonon frequency, the dielectric constant approaches unity and impedance mismatch between free space and the PC antenna (The static dielectric constants of InP and GaAs are 13 and 12.6, respectively) is alleviated. This results in higher signal strengths near these frequencies. The spectral dip observed around 5 THz is due to the transverse optical (TO) phonon (ω_{TO}=5.3 THz) in the ZnTe emitter. We also observe strong absorption at frequencies of TO phonons of InP (9.1 THz) and GaAs (8 THz). The origin of the peak around 13 THz is not clear. It may be associated with a water vapor absorption line at 12 THz.[16] The spectral dip observed at 15 THz is attributed to the absorption due to a oxygen impurity mode (The ν_2 bending mode of O_2 molecules around 15.5 THz)[17] in the Si plate used as the beam combiner for THz and optical probe beams. The dip at 18 THz is attributed to the two phonon (TO(L) + TA(L) or TO(X) + TA(X)) absorption in the Si beam combiner.

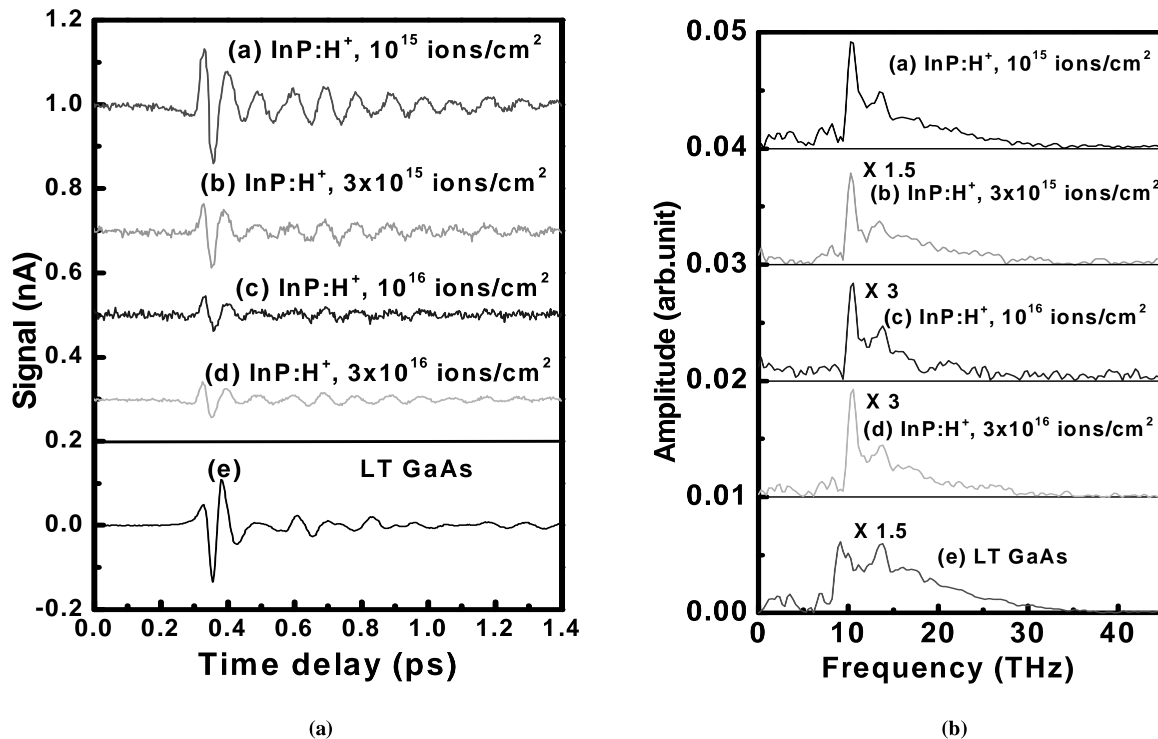

Fig. 7. (a) The THz waveforms and the corresponding Fourier transformed amplitude spectra (b) detected by each InP: H^+ and the LT-GaAs PC antenna

Downloaded From: http://proceedings.spiedigitallibrary.org/ on 04/26/2014 Terms of Use: http://spiedl.org/terms

The high frequency ends of the spectral distribution for the LT-GaAs and InP:H^+ PC antenna are also summarized in Table 2. The bandwidth of the PC antennas is mainly limited by the laser pulse width.[18] The detectable frequency components at high frequency side are also limited by the noise level in the PC antennas. It was reported that the main contribution to the noise in a PC detector is the Johnson noise (or thermal noise in resistance) and the laser shot noise[8]. The Johnson noise in current is inversely proportional to the square-root of the resistance, $1/\sqrt{R}$, while the laser shot noise is dependent on the laser power but not on the material properties of the PC substrate. The photoconductive resistance is inversely proportional to the conductivity, σ, which in turn is proportional to product of mobility, μ, and carrier life time, τ. As the result, the noise level is proportional to square root of the product of carrier life time and mobility: $I_{noise} \propto 1/\sqrt{R} \propto \sqrt{\sigma} \propto \sqrt{\mu\tau}$. The similarity between the spectra obtained with all of PC antennas indicates that neither the carrier life time nor the mobility (the carrier momentum relaxation time, in other words) are critical parameters for the detection bandwidth of the PC antenna although these material parameters determine the efficiency and noise properties of the PC antennas.

We have plotted the noise of various PC antennas against $1/\sqrt{R}$ in Fig. 8 The noise data fit well with a linear dependence, $J_{noise} = y_0 + m \times 1/\sqrt{R}$, with a slope of m = 175 and an offset $y_0 = 0.3$ in the scale of Fig. 8. In the limit of high resistance the only contribution to the noise is the laser shot noise, which is given by the offset parameter y_0. The small y_0 indicates the noise in our PC antennas is dominated by the Johnson noise. The SNRs of the InP:H^+ PC antenna, which are given by the ratios of spectral peak amplitude and the noise level, are summarized in Table 1. Although the low resistivity of InP: H^+ resulted in the high noise level, its high photoconductive gain partly compensates this drawback. An example is the SNR of the PC antenna using InP: H^+(10^{15} ion/cm^2), which was about half of that with the LT-GaAs antenna, despite of the unfavorable resistivity ratio $\sqrt{R(InP:H^+)/R(LT-GaAs)}$ ~ 1/30.

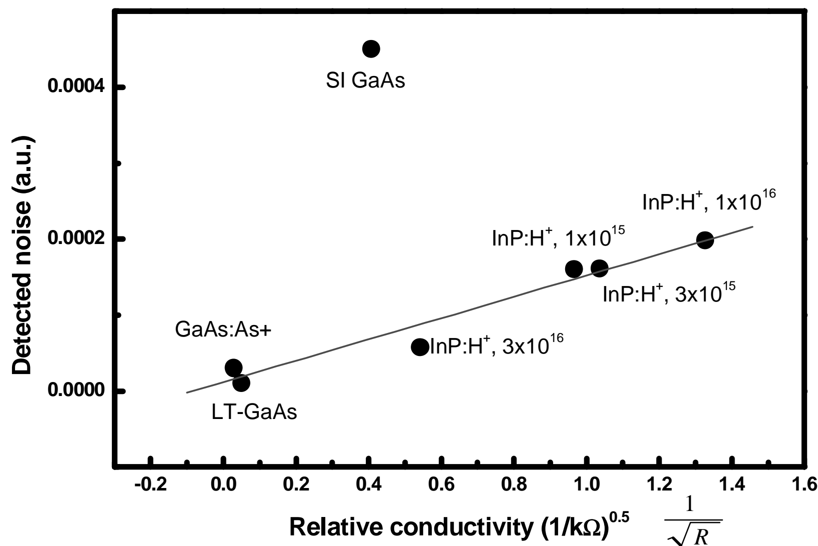

Fig. 8. Noise level of different InP: H^+ samples, SI-GaAs, GaAs:As^+ and LT-GaAs PC antenna are plotted as a function of conductance. Circle dot is the data point, dashed line is the fitting curve.

SUMMARY

In summary, we have investigated the performance of GaAs: As^+ and InP: H^+ PC antennas as ultrabroadband THz wave detector. With THz radiation generated from a thin ZnTe emitter excited by 15-fs optical pulses, the

Downloaded From: http://proceedings.spiedigitallibrary.org/ on 04/26/2014 Terms of Use: http://spiedl.org/terms

detectable frequency distribution was confirmed to be about 30 THz. Although the SNR with $GaAs:As^+$ PC antenna was lower than that of LT-GaAs PC antenna, it is possible to improve the efficiency by increasing the ion-implanted layer thickness. The peak THz signal of the $InP:H^+$ (10^{15} ions/cm^2) PC antenna is slightly higher than that of the LT-GaAs one, while the SNR of the former is about half as high as the latter. This can be improved by increasing the resistivity of $InP:H^+$ through optimizing the ion dosage level and/or the annealing condition. Our results indicate both $GaAs:As^+$ and InP: H^+, and other ion-implanted III-V photocoudctors could be developed into promising materials as the photoconductive substrate for ultrabroadband PC antennas.

ACKNOWLEDGEMENTS

The author would like to acknowledge and thank his colleagues and collaborators, M. Hangyo, M. Tani, T. A. Liu for their contributions in this work. Ci-Ling Pan was supported by the National Science Council and the Ministry of Education of the ROC under various grants.

REFERENCES

1. P. Q. Wu, and X. -C. Zhang, Appl. Phys. Lett. **71,** 1285 (1997).
2. R. Huber, A. Brodschelm, F. Tauser, and A. Leitenstorfer, Appl. Phys. Lett. **76,** 3191 (2000).
3. S. Kono, M. Tani, and K. Sakai, Appl. Phys. Lett. **79**, 898 (2001).
4. S. Kono, M. Tani, Ping Gu, and K. Sakai, Appl. Phys. Lett. **77**, 4104 (2000).
5. S. Kono, M. Tani, and K. Sakai, IEE. Proc. Optoelectron. **149**, 105 (2002).
6. F. Ganikhanov, G. -R. Lin, and C. -L. Pan, Appl. Phys. Lett. **67,** 3465 (1995).
7. A. Claverie, F. Namavar, and Z. Liloental-Weber, Appl. Phys. Lett. 62, 1271(1993).
8. M. Tani, K. Sakai and H. Mimura, Jpn. J. Appl. Phys. **36**, 1175 (1997).
9. B. W. Liang, P. Z. Lee, D. W. Shih, and C. W. Tu, Appl. Phys. Lett. **60**, 2104 (1992).
10. K. F. Lamprecht, S. Juen, L. Palmetshofer, and R. A. Höpfel, Appl. Phys. Lett. **59**, 926 (1991).
11. C. Messner, H. Kostner, R. A. Höpfel, and K. Unterrainer, J. opt. Soc. Am. B. **18**, 1369, (2001).
12. T. A. Liu, M. Tani, M. Nakajima, M. Hangyo and C. L. Pan, Appl. Phys. lett. **83**, 1322 (2003).
13. T. A. Liu, M. Tani, M. Nakajima, M. Hangyo, K. Sakai , S. Nakashima, and C. L. Pan, Optics Express, **12**, 2954 (2004).
14. H. Boudinov, J.P. De Souza, and C. Jagadish, Nucl. Instr. And Meth. B. **175**, 235 (2001).
15. G. R. Lin, W. C. Chen, S. C. Chao, C. S. Chang, K. H. Wu, T. M. Hsu, W. C. Lee, and C. L. Pan, IEEE J. Quantum Electron. **34**, 1740 (1998).
16. A. R. H. Cole, *Tables of Wave numbers for the Calibration of Infrared Spectrometers* (Pergamon, Oxford, 1977).
17. K. Nakamoto, *Infrared and Raman Spectra of Inorganic and Coordination Compounds, 4th edition* (Wiley, New York 1986), pp. 474.
18. L. Duvillaret, F. Garet, J-F. Roux, and J-L. Coutaz, IEEE J. Sel. Top. Quantum Electron. **7**, 615 (2001).

Downloaded From: http://proceedings.spiedigitallibrary.org/ on 04/26/2014 Terms of Use: http://spiedl.org/terms